THz wave transmission within the metal film coated double-dielectric-slab waveguides and the tunable filter application

Jiamin Liu[a,b,c], Huawei Liang[b, c]*, Min Zhang[b, c] and Hong Su[b, c]

[a]College of Electronic Science and Technology, Shenzhen University, Shenzhen, 518060, China

[b]Shenzhen Key Laboratory of Laser Engineering, Shenzhen University, Shenzhen, 518060, China

[c]Key Laboratory of Advanced Optical Precision Manufacturing Technology of Guangdong Higher Education Institutes, Shenzhen University, Shenzhen, 518060, China *Corresponding author: hwliang@szu.edu.cn

Abstract: We propose a metal film coated double-dielectric-slab waveguide for guiding THz wave. Detailed comparisons of transmission characteristics of the coated and uncoated double-dielectric-slab waveguides are given. The comparisons of different slab materials are also given. We put forward using the measureable cut-off frequency of the coated waveguides for tunable filter. The tunable sensitivities to the thickness of the slab t and the air interval w are discussed. We find that for Polystyrene slab at t = 0.0380 mm, the theoretical tunable sensitivity of cut-off frequency on w can be 7.65 THz/mm.

Key words: Waveguides; Infrared, far; Waveguides, planar

1. Introduction

In recent years, THz waveguides [1,2,3] have been widely studied, such as metal wire waveguides [4-6], dielectric pipe waveguides [7-10], ultra-thin metal pipe waveguides [11]. Since they are first proposed, various applications of them have been studied and reported, such as transmission, sensing [12,13], filtering. Among these cylindrical waveguides, the metal waveguides are most based on surface plasmon and the dielectric pipe waveguides are based on anti-resonant reflecting. However, both these two kinds of waveguide are based on the propagation of a large portion of field in air, and the coupling efficiency of metal wire waveguides is low (43.5% in reference [14]). Recently, research interests on planar THz waveguides [2,3] have been paid much attention, such as parallel plate waveguides [15-17], metal nanofilm waveguides [18], metal-clad hollow waveguides [19], and single metal plate waveguides [20-23]. For their simple structure, low loss, high coupling efficiency and good confinement of mode field, such waveguides are more commonly used in transmission [15-17], sensing [20-25], filtering [19, 26-28]. For the development to applications, THz filters are important devices, there still needs more filters on THz field, and the detecting of metal films on dielectric surface is not discussed yet.

In this paper, we propose using metal film coated double-dielectric-slab waveguide for guiding THz wave. We have derived the dispersion equation of the TE mode of the waveguides and numerically study the relationships between the propagating characteristics and the THz wave frequency, as well as the waveguide structure. The mode field distribution characteristics of the TE mode are also studied. In transmission aspects, the detailed comparing between coated and uncoated Polystyrene (PS) waveguide is given and the detecting of metal films on dielectric slab surfaces is also discussed. The comparisons of different slab materials are also given. In aspects of applications, we put forward using the measureable cut-off frequency of the coated waveguide for tunable filter. The tunable sensitivities to the thickness of the slab t and the air interval w are discussed. We believe that these results are very

useful for designing of THz waveguides, sensors, and filters.

2. The dispersion equation of metal film coated double-dielectric-slab waveguide

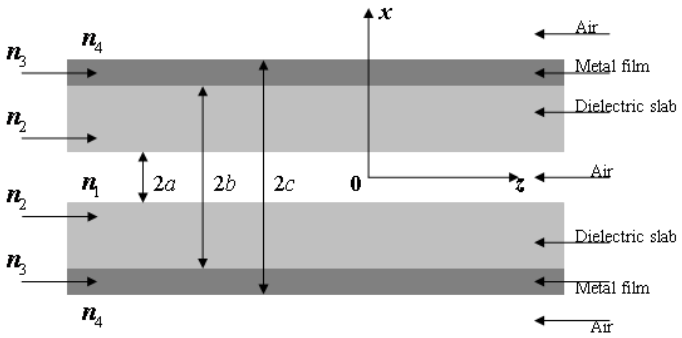

Fig. 1 The structure of the metal film coated double-dielectric-slab waveguide

TE mode of THz wave transmits in the *z*-direction in metal film coated double-dielectric-slab waveguide, as shown in Fig. 1. $w = 2a$ is the air interval between the two dielectric slabs. $t = b - a$ is the thickness of each slab. $d = c - b$ is the thickness of metal film. The metal films coated here are very thin and lower than the penetration depth of THz wave to metal, so the mode field in the 7 layers should be considered as an unity. We only consider the boundary of the *x*-direction, and the width on *y*-direction is big enough, thus the TE mode field components can be written as [29]:

$$E_y(x) = \begin{cases} A_{10}e^{-h_4(x-c)} & x \ge c \\ A_6 e^{-h_3(x-b)} + A_7 e^{h_3(x-b)} & b \le x \le c \\ A_2 \cos h_2(x-a) + A_3 \sin h_2(x-a) & a \le x \le b \\ A_1 \cos(h_1 x) & -a \le x \le a \\ A_4 \cos h_2(x+a) + A_5 \sin h_2(x+a) & -b \le x \le -a \\ A_8 e^{-h_3(x+b)} + A_9 e^{h_3(x+b)} & -c \le x \le -b \\ A_{10}e^{h_4(x+c)} & x \le -c \end{cases} \quad (1)$$

where $h_1 = (n_1^2 k_0^2 - \beta^2)^{1/2}$, $h_2 = (n_2^2 k_0^2 - \beta^2)^{1/2}$, $h_3 = (\beta^2 - n_3^2 k_0^2)^{1/2}$, and $h_4 = (\beta^2 - n_4^2 k_0^2)^{1/2}$. $\beta = \beta_1 - j*\alpha$ is the complex variable, in which the real part β_1 is related to the effective refractive index $n_{eff} = \beta_1 / k_0$ and the imaginary part α is the loss coefficient of the guiding mode which include all the losses in the 7 layers. $k_0 = 2\pi / \lambda$ is the wave vector in vacuum, and n_1, n_2, n_3, and n_4 are refractive indices of air, PS slab, metal film and air, respectively. According to the boundary conditions of the waveguide, the dispersion equation of TE mode can be derived as [29]:

$$\tan(h_1 a) = \frac{P_1 + P_2}{P_3 + P_4} \quad (2)$$

where $P_1 = [1 + \frac{h_2}{h_3}\tan h_2(b-a) - \frac{h_3}{h_4} - \frac{h_2}{h_4}\tan h_2(b-a)]e^{-h_3(c-b)}$,

$$P_2 = [1 - \frac{h_2}{h_3}\tan h_2(b-a) + \frac{h_3}{h_4} - \frac{h_2}{h_4}\tan h_2(b-a)]e^{h_3(c-b)},$$

$$P_3 = [-\frac{h_3}{h_4}\frac{h_1}{h_2}\tan h_2(b-a) + \frac{h_1}{h_4} + \frac{h_1}{h_2}\tan h_2(b-a) - \frac{h_1}{h_3}]e^{-h_3(c-b)}, \text{ and}$$

$$P_4 = [\frac{h_3}{h_4}\frac{h_1}{h_2}\tan h_2(b-a) + \frac{h_1}{h_4} + \frac{h_1}{h_2}\tan h_2(b-a) + \frac{h_1}{h_3}]e^{h_3(c-b)}.$$

Copper is adopted as the material of the metal film, and its relative permittivity $\varepsilon_3 = n_3^2$ can be gotten according to the Drude model [30]. The materials of dielectric slabs are chosen as Polystyrene (PS) with a refractive index of $n_2 = 1.58 - j0.0036$ [31] or silicon. The refractive index of air is $n_1 = n_4 = 1.$

3. The transmission characteristics of metal film coated double-dielectric-slab waveguide

3.1 Relationships between transmission characteristics and THz frequency (PS slabs)

When the metal film thickness is d = 1 nm, the air interval between two slabs is w = 0.3 mm, and the thickness of a slab is t = 0.5 mm, we numerically calculate the dependence of the loss coefficient on the THz frequency by Eq. (2), as shown in Fig. 2(a) solid line, and the dashed line is corresponding to d = 0. We find that not only the loss has been increased after coating but also the change law is significantly different. The loss of uncoated double-dielectric-slab waveguide increases monotonously with the increasing of frequency. This is because when the THz wavelength is smaller, more energy will distribute in the high loss PS slabs, and less in the air. While there is a low frequency cut-off in the coated waveguide. Losses near the cut-off frequency have increased dramatically and at the middle frequency of f = 0.25 THz, there appears a minimum loss $\alpha = 0.392\text{cm}^{-1}$. The minimum loss happens because at this point, the energy in the metal films is the least. In the parallel plate waveguides there is a low cut-off frequency of TE mode [15, 16]. Here the cause of cut-off frequency of the coated waveguide has a similar mechanism. As shown in the inset, inside the waveguide, the propagation constant can be written as $\beta = \sqrt{\beta_x^2 + \beta_z^2}$, and [15]: $\cos\theta = \frac{\beta_x}{\beta} = \frac{mc}{2(2n_2 t + w)f}$, where m = 1, 2, 3..., $c = 3\times10^8 m/s$ is the speed of light in vacuum, n_2t is the optical thickness of a PS slab. When the propagation constant only has x components, the mode will be cut-off and $\theta = 0$. So we get the cut-off frequency of TE_m mode as:

$$f_{cm} = \frac{mc}{2(2n_2 t + w)} \tag{3}$$

By using Eq. (3), we get the TE_1 mode cut-off frequency of this condition is $f_{c1} = 0.08\text{THz}$, and at

this frequency, the loss is $\alpha = 8.15\,\mathrm{cm}^{-1}$ which is about 21 times of the minimum loss. Further reducing the frequency, the loss will increase dramatically (such as the loss is $\alpha = 19.5\,\mathrm{cm}^{-1}$ at 0.05 THz). However, the loss of the uncoated waveguide at this low frequency is extremely low. With the increase of frequency, after the minimum loss point, the loss of the coated and uncoated waveguides are coming to the same law, which tells us that the effect of metal films on the loss of double-dielectric-slab waveguides is weaker in the higher frequency. Because when the THz wavelength is smaller, the waveguide structure is much larger than the THz wavelength, and the effects of dielectric slabs will be more obvious for the size of the slabs is much bigger than the metal films.

According to the equation $v_g = \dfrac{c}{n_{eff}\left(1+\dfrac{k_0}{n_{eff}}\dfrac{\mathrm{d}n_{eff}}{\mathrm{d}k_0}\right)}$, we obtain the relationship of the group velocity varying with the frequency of both the two kinds of waveguides, as shown in Fig. 2 (b). We can know that the group velocity dispersion (GVD) increases sharply near the cut-off frequency after coating, for much more energy distributing in the metal films. While the GVD of the uncoated waveguide is relatively uniform in the given range of THz frequency. The group velocity of the uncoated waveguide is decreasing as the frequency increasing, which is also because there is more THz wave energy distributing in the PS slabs as the frequency increasing. The group velocity of the coated waveguide is smaller, for after coating there will be more energy in the PS slabs and some in the metal films, which causes less energy in the low loss air. The effect of metal films on group velocity of the waveguide is also much lower in higher frequencies. Based on the high GVD near the cut-off frequency after coating, we can detect the thin metal films on the dielectric slab surface.

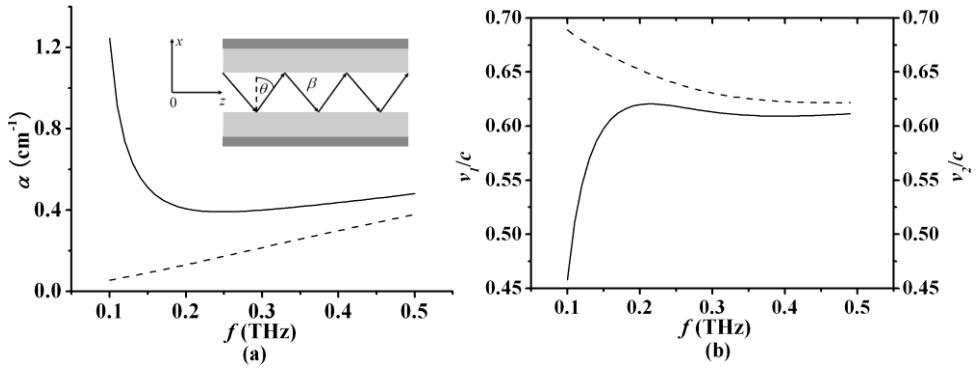

Fig.2 (a) The dependence of loss on THz frequency of coated (solid line) and uncoated (dashed line) waveguides, inset is the longitudinal cross section of the coated waveguide depicting the bouncing plane wave. (b) The dependence of group velocity on THz frequency of coated (solid line) and uncoated (dashed line) waveguides.

3.2 Relationships between transmission characteristics and the thickness of metal film (PS slabs)

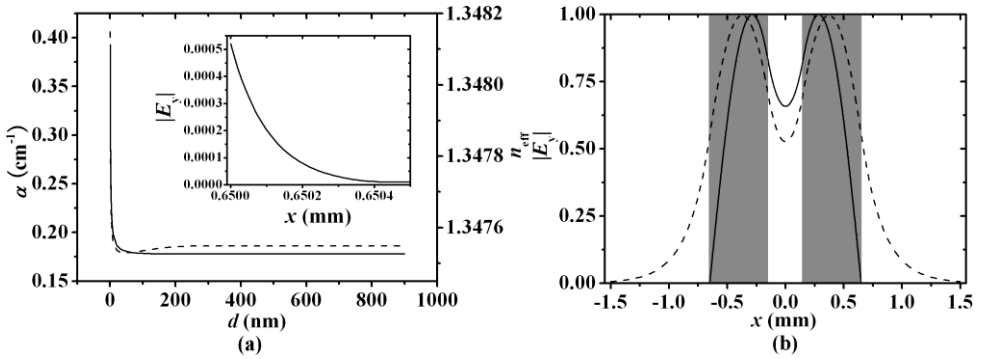

Fig.3 (a) The dependence of loss on the thickness of metal film (solid line) and the corresponding effective refractive index (dashed line), inset is mode field distribution in the metal film of d = 500 nm. (b) The mode field distribution of coated (solid line) and uncoated (dashed line) waveguides, the gray regions are the positions of the slabs.

When THz frequency is f = 0.25 THz, the air interval between the two slabs is w = 0.3 mm, and the thickness of the slab is t = 0.5 mm, we get the relationship between the loss and the film thickness, as shown in Fig. 3 (a) solid line, dashed line is the corresponding effective refractive index. The figure shows that when the coated films are very thin, the loss is very big and reduces sharply with the increase of film thickness. This is because even though the films are thinner, the amplitude of the mode field in the metal films is larger (for example it is more than 0.04 for d = 1 nm, however, it is only 0.0005 for d = 500nm, as shown in the inset). When the films are thicker, the loss tends to be an unchanged value. According to Eq. (1), we get the mode field distribution in the metal films when d = 500 nm, as shown in the inset. By the inset, we can see that the penetration depth of THz wave to the metal is small, at the film thickness of 500 nm, THz wave cannot penetrate through the metal films.

Figure 3 (b) is derived when THz frequency is f = 0.25 THz, the air interval between the two slabs is w = 0.3 mm, the thickness of the slab is t = 0.5 mm, and the metal film thickness is d = 10 nm (solid line) and d = 0 (dashed line). Fig. 3 (b) illustrates that the mode field width decreases after coating, however the loss increases only a little for thick slab (here t = 0.5 mm), and they are $\alpha = 0.198\text{cm}^{-1}$ (d = 10 nm), $\alpha = 0.172\text{cm}^{-1}$ (d = 0 nm), respectively. Because the slab is relatively thicker and the absorption loss of the PS is high, the adding of metal films causes relatively lower loss, which also tells us that the effects of metal films are also lower for this case.

3.3 Relationships between transmission characteristics and the air interval between the two slabs (PS slabs)

When the THz frequency is f = 0.25 THz, film thickness is d = 10 nm, and the thickness of a slab is t = 0.5 mm, the law of the loss changing with air interval between the coated (solid line) and uncoated (dashed line) two slabs are derived and shown in Fig. 4 (a). By the figure we can know that for the thick slab (here t = 0.5 mm), the law of loss changing with w is basically the same of both the coated and the uncoated waveguides. They both have a minimum loss point, and it is at about w = 0.26 mm in this case. Because the adding of metal films has little effect on the distribution of the field in the air interval between the two slabs. It is worth to point out that in this case at w = 0.26 mm, the effects of metal films on the loss of the double-dielectric-slab are the weakest, this is important for designing the structure of the waveguide. In order to explain this phenomenon, we get the mode field distribution of the coated waveguide at w = 0.26 mm (solid line) and w = 0.6 mm (dashed line) when f = 0.25 THz, d = 10 nm, and t = 0.5 mm, as shown in Fig. 4 (b). Fig. 4 (c), (d) are the mode field in the metal films

respectively. By the figure, we can see when the air interval between two slabs is w = 0.26 mm, not only the percentage of mode energy in the air interval increases but also the percentage of mode energy in the metal film decreases, so the loss is lower. When w is smaller, the cut-off frequency of the waveguide increases, which makes 0.25 THz closer to the cut-off frequency, thus the loss increases.

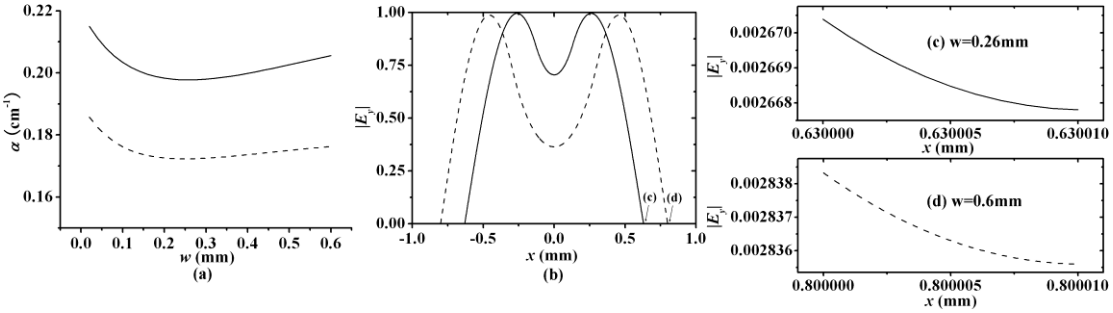

Fig.4 (a) The dependence of loss on air interval between two slabs of coated (solid line) and uncoated (dashed line) waveguides. (b) The mode field distribution of w = 0.26 mm (solid line) and w = 0.6 mm (dashed line) in the waveguides, (c) (d) are mode field distributions in the metal films of w= 0.26 mm and w = 0.6 mm, respectively.

3.4 Relationships between transmission characteristics and the thickness of a slab (PS slabs)

When the THz frequency is f = 0.25 THz, the film thickness is d = 10 nm, the interval between two slabs is w = 0.3 mm, the laws of the loss changing with the thickness of a slab of coated (solid line) and uncoated (dashed line) waveguides are derived and shown in Fig. 5 (a). We can see that the loss of the coated waveguide decreases monotonously with the increasing of the slab thickness (the loss is $\alpha = 0.197\text{cm}^{-1}$ for t = 0.6 mm), while the loss of the uncoated waveguide increases monotonously with the increase of the slab thickness for more energy in thicker slabs. It is worth to point out that the effects of the metal films are much weaker when the thickness of the slab is thicker. This is because the thicker the PS slabs are, the effects of PS slabs are more obvious. After coating, there appears a cut-off slab thickness, its value can be derived by Eq. (3) as:

$$t = \frac{1}{n_2}\left(\frac{c}{4f_c} - \frac{w}{2}\right) \tag{4}$$

Substituting the values into Eq. (4), we get the cut-off thickness is 0.095 mm in this case, at this point its loss is $\alpha = 31.23\text{cm}^{-1}$, which is 158 times of the loss of t = 0.6 mm.

We also get the mode distribution at a lower slab thickness (t = 0.01 mm) of coated (solid line) d = 10 nm and uncoated (dashed line) d = 0 nm waveguides when f = 0.25 THz, and w = 0.3 mm, as shown in Fig. 5 (b). Figure illustrates that the difference of mode field width (amplitude decay as 1/e) is huge. In the uncoated waveguide, the mode field has a great extension in the outside air, and the mode field width is about 6 mm. However, after coating, the mode field is confined in the air interval between the two slabs, and the mode field width is about 0.3 mm, which is only 1/20 of the uncoated waveguide. On the basis of this, we can detect the presence of metal films on the surface of the thin dielectric slabs through the significance difference on energy concentration. And in this case, the uncoated loss is $\alpha = 0.00205\text{cm}^{-1}$. However, the loss of the coated waveguide is $\alpha = 83.0\text{cm}^{-1}$ which is more than 40000 times larger. So based on the huge differences on the loss, we can also detect the presence of metal films on thin slabs. Fig. 5(c) shows that a significant increased mode field energy is in the

metal films compared with t = 0.5 mm (Fig. 4 (c) and (d)) which contributes the huge loss. In the case of very thin dielectric slabs, we can change w, if we can get a huge loss, it can be concluded a presence of metal films on dielectric slabs.

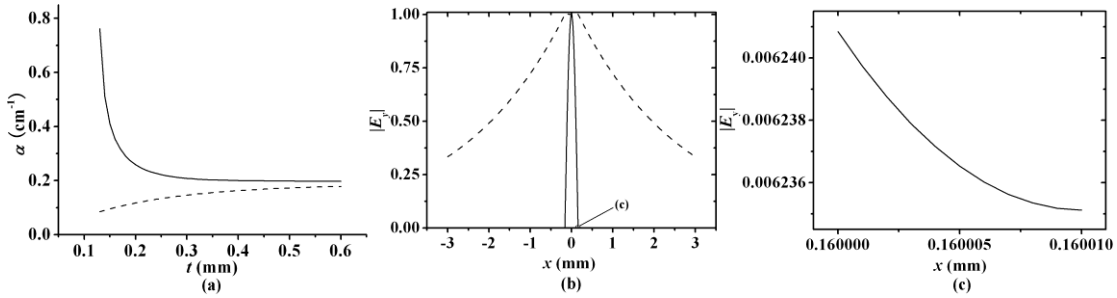

Fig.5 (a) The dependence of loss on slab thickness of coated (solid line) and uncoated (dashed line) waveguides. (b) The mode field distribution of t = 0.01 mm in coated (solid line) and uncoated (dashed line) waveguides. (c) is the mode field distribution in the metal film.

3.5 Relationships between transmission characteristics and the THz frequency for silicon slabs

We keep the parameters of the waveguide the same as Section 3.1 (d = 1 nm, w = 0.3 mm, t = 0.5 mm), however, we choose silicon as the material of the two slabs, and we get the change law of loss to THz frequency and the corresponding mode field distribution, as shown in Fig 6. The refractive index of the silicon is $n_2 = \sqrt{\varepsilon_2}$, and the relative dielectric constant of silicon ε_2 can be calculated by the Drude model [30]:

$$\varepsilon_2 = \varepsilon_\infty - \frac{\omega_p^{\,2}}{\omega^2 - i\omega\omega_\tau} \tag{5}$$

where $\varepsilon_\infty = 11.7$ is the high frequency dielectric constant, ω_p is the plasma oscillation frequency, ω_τ is the damping frequency, and ω is the angular frequency of the THz wave. Here we adopt the low doped silicon which has a parameter as $\omega_p = 0.01\times10^{12}$ Hz, $\omega_\tau = 0.67*10^{12}$ Hz.

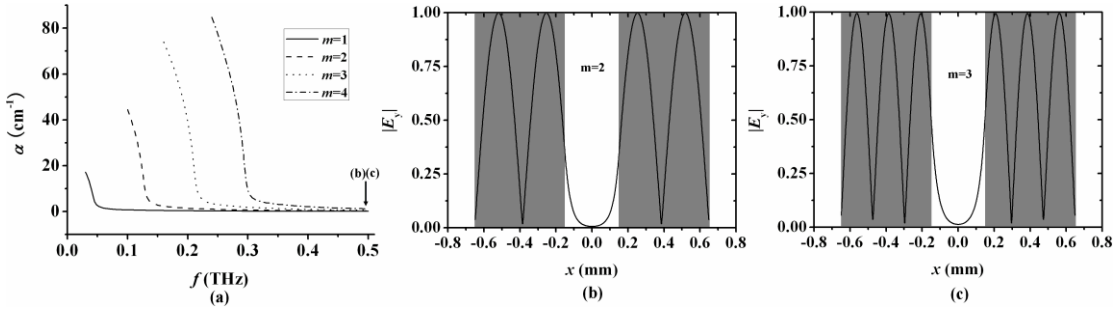

Fig.6 (a) The dependence of loss on THz frequency of coated silicon slab waveguides, from left to right the curves are corresponding to the TE_1, TE_2, TE_3, TE_4 mode, respectively. (b) and (c) are the mode field distribution of coated silicon slab waveguides when f = 0.5 THz, m = 2 or 3, respectively, the gray regions are the positions of the slabs.

Figure 6 (a) shows that even though the parameters of the silicon waveguide is the same as the PS waveguide in Section 3.1, multiple modes appear in the range from 0 – 0.5 THz in the silicon

waveguide, and the single mode transmission range is narrower. For the refractive index of the silicon is $n_2 = \sqrt{11.7} = 3.42$, which is much larger than that of the PS slab, the optical interval between the two metal films is much larger and the cut-off frequency of TE_1, TE_2, TE_3, TE_4 mode is much smaller (0.04 THz, 0.08 THz, 0.12 THz, 0.16 THz, respectively). Moreover, the mode loss is much larger than the PS waveguide, even though the absorption coefficient (the imaginary part of the relative dielectric constant) of this low doped silicon is only $\sim 10^{-6}$ which is more than 4 orders of magnitude larger than the absorption coefficient of PS. The high refractive index of the silicon makes the THz wave much easier for total internal reflection on the interface of the silicon slab, which makes much more energy distribute in the silicon slabs (as shown in Fig. 6 (b) and (c)). As the tangential components of the electromagnetic fields on interfaces are continuous, the energy distributing in the metal films will also be much larger, which contributes the larger loss. Figure 6 (b) and (c) also show that the number of field peaks are 2 and 3 for m = 2 and 3, respectively.

4. The tunable filter applications

Because the loss will increase sharply and be huge at the cut-off frequency, and the cut-off frequency can be modified by changeable w, the waveguide can be used for tunable high-pass filter. According to Eq. (3), the cutoff frequency is determined by both t and w. In case of a fixed t, the changing of w will move the cut-off frequency. So the changing of f_{c1} has a tunable sensitivity to w, and it can be represented as:

$$S = \left| \frac{\mathrm{d}f_{c1}}{\mathrm{d}w} \right| = \frac{c}{2(2n_2 t + w)^2} \tag{6}$$

In the case of t = 0.316 mm (optical thickness $n_2 t$ = 0.5 mm), according to Eq. (3) and Eq. (6), we have gotten the cut-off frequency and the tunable sensitivity of cut-off frequency on w, as shown in Fig 7 (a) :

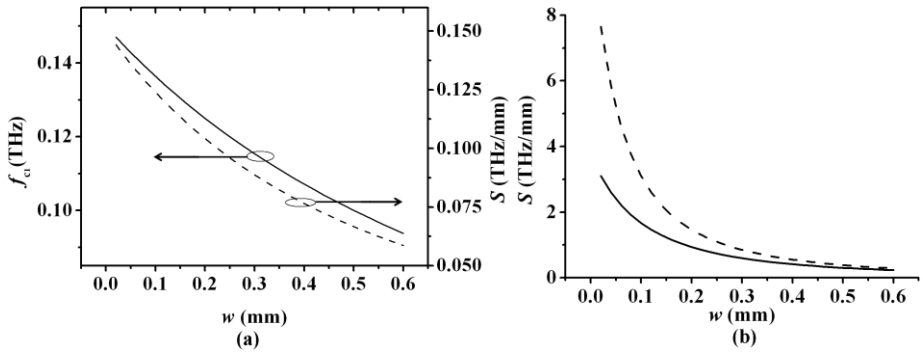

Fig. 7 (a) The dependence of cut-off frequency (solid line) and tunable sensitivity of cut-off frequency (dashed line) on air interval w between the two slabs. (b) The dependence of tunable sensitivity of cut-off frequency on w when t = 0.1 mm (solid line) and t = 0.06 mm (dashed line).

By Fig. 7 (a), we can see that both the cut-off frequency and the tunable sensitivity of cut-off frequency on w decrease with the increasing of w. For t = 0.316 mm, the changing of cut-off frequency is not big, and the tunable sensitivity is below 0.144 THz/mm. In order to know the influence of t on the tunable sensitivity, we also get the tunable sensitivity at t = 0.0633 mm ($n_2 t$ = 0.1 mm, solid line) and 0.0380 mm ($n_2 t$ = 0.06 mm, dashed line) as a function of w, as shown in Fig. 7 (b). The figure shows that when

the slab thickness is reduced, the tunable sensitivity increases significantly, and at t = 0.0380 mm the tunable sensitivity can reach 7.65 THz/mm at w = 0.02 mm. It is worth to point out that single mode transmission is much better for filter application, so PS is more proper than silicon to be chosen as the material of the slabs.

5. Conclusions

In conclusion, we propose using metal film coated double-dielectric-slab waveguide for guiding THz wave. In transmission aspects, we find that after coating, the TE modes of the waveguide appear a low cut-off frequency which is nonexistent before coating. Both the loss and the dispersion increase sharply near the low cut-off frequency. For thick PS slab the loss increase a little but the mode field width reduces significance after coating. For thin PS slab, the mode field width decreases greatly and the loss can be more than 40000 times larger after coating. The material of silicon for dielectric slabs is also discussed. The In aspects of applications, We find that the theoretical tunable sensitivity of cut-off frequency on w decreases with the increase of w, and obviously increases with the decrease of t. At t = 0.0380 mm, the tunable sensitivity of cut-off frequency on w can be 7.65 THz/mm.

Acknowledgments

This work was supported in part by the National Natural Science Foundation of China under Grant 61405124, Natural Science Foundation of Guangdong Province, China under Grant 2014A030313560, the Specialized Research Fund for the Doctoral Program of Higher Education of China under Grant 20134408120002, and the Fund Project for Shenzhen Fundamental Research Programme under Grant JCYJ20130329140707824.

References

[1] G. Gallot, S. P. Jamison, R.W. McGowan, and D. Grischkowsky, “Terahertz waveguides,” J. Opt. Soc. Am. B 17, 851-863 (2000).

[2] S. Atakaramians, S. Afshar V., T. M. Monro, and D. Abbott, “Terahertz dielectric waveguides” Advances in Optics and Photonics 5, 169–215 (2013).

[3] M. Nagel, A. Marchewka, and H. Kurz, "Low-index discontinuity terahertz waveguides," Opt. Express 14, 9944-9954 (2006).

[4] K.Wang, and D. M. Mittleman, “Metal wires for terahertz waveguiding”, Nature 432, 376 (2004).

[5] K. Wang, and D. M. Mittleman, “Dispersion of surface plasmon polaritons on metal wires in the terahertz frequency range”, Phys. Rev. Lett 96, 157401 (2006).

[6] T. Jeon, J. Zhang, and D. Grischkowsky, “THz Sommerfeld wave propagation on a single metal wire”, Appl. Phys. Lett 86, 161904 (2005).

[7] C.-H. Lai, Y.-C. Hsueh, H.-W. Chen, Y.-J. Huang, H.-C. Chang, and C.-K. Sun, “Low-index terahertz pipe waveguides,” Opt. Lett. 34, 3457-3459 (2009).

[8] C.-H. Lai, B. You, J.-Y. Lu, T.-A. Liu, J.-L. Peng, C.-K. Sun, and H. C. Chang, “Modal characteristics of antiresonant reflecting pipe waveguides for terahertz waveguiding,” Opt. Express 18, 309-322(2010).

[9] J.-T. Lu, Y.-C. Hsueh, Y.-R. Huang, Y.-J. Hwang, and C.-K. Sun, “Bending loss of terahertz pipe waveguides,” Opt. Express 18, 26332–26338 (2010).

[10] E. Nguema, D. Fèrachou, G. Humbert, J. L. Auguste, and J. M. Blondy, “Broadband terahertz transmission within the air channel of thin-wall pipe,” Opt. Lett. 36, 1782–1784 (2011).

[11] H. W. Liang, S. C. Ruan, M. Zhang, H. Su and I. L. Li, “Surface plasmon-polaritons on very thin metal tubes” Opt. Express 23, 125001 (2013).

[12] M. Wächter, M. Nagel, and H. Kurz, "Frequency-dependent characterization of THz Sommerfeld wave propagation on single-wires," Opt. Express 13(26), 10815–10822 (2005).
[13] Nick C. J. van der Valka and Paul C. M. Planken, "Effect of a dielectric coating on terahertz surface plasmon polaritons on metal wires," Appl. Phys. Lett. 87, pp071106 (2005).
[14] J. Liu, H. Liang, M. Zhang, and H. Su, "Coupling of Sommerfeld waves using odd TM mode of double-dielectric-slab waveguide," J Opt 44(1), 53–58 (2014).
[15] R. Mendis and D. M. Mittleman, "An investigation of the lowest-order transverse-electric (TE1) mode of the parallel-plate waveguide for THz pulse propagation," J. Opt. Soc. Am. B 26, A6-A13 (2009).
[16] R. Mendis and D. M. Mittleman, "Comparison of the lowest-order transverseelectric (TE1) and transverse-magnetic (TEM) modes of the parallel-plate waveguide for terahertz pulse applications," Opt. Express 17, 14839-14850 (2009).
[17] J. Liu, H. Liang, M. Zhang, and H. Su, "Broadband terahertz transmission within the symmetrical plastic film coated parallel-plate waveguide" App. Opt. 53(26), 6008-6012 (2014).
[18] H. W. Liang, S. C. Ruan, M. Zhang, H. Su and I. L. Li , "Characteristics of modified surface plasmon polaritons on double-coated metal nanofilms" Laser Phys. Lett. 11, 115003 (2014).
[19] J.-Y. Lu, H.-Z. Chen, C.-H. Lai, H.-C. Chang, B. You, T.-A. Liu, and J.-L. Peng, "Application of metal-clad antiresonant reflecting hollow waveguides to tunable terahertz notch filter," Opt. Express 19(1), 162–167 (2011).
[20] M. Gong, T.-I. Jeon, and D. Grischkowsky, "THz surface wave collapse on coated metal surfaces" Opt. Express 17(19), 17088-17101 (2009).
[21] J. Saxler, J. G. Rivas, C. Janke, H. P. M. Pellemans, P. H. Bolı´var, and H. Kurz, "Time-domain measurements of surface plasmon polaritons in the terahertz frequency range" Phys. Rev. B 69, 155427 (2004).
[22] T. H. Isaac,W. L. Barnes, and E. Hendry, "Determining the terahertz optical properties of subwavelength films using semiconductor surface plasmons" Appl. Phycs. Lett. 93, 241115 (2008).
[23] J. Liu, H. Liang, M. Zhang, and H. Su, "Metal plate for guiding terahertz surface plasmon-polaritons and its sensing applications" Opt. Communications **339** 222–227 (2014).
[24] H. Liang, S. Ruan, S. Xu, M. Zhang, H. Su, and I. L. Li, "Modified surface plasmon polaritons with ultrahigh figures of merit on metal-gap–dielectric waveguides" Applied Physics Express 7, 122001 (2014).
[25] R. Mendis, V. Astley, J. Liu, and D. M. Mittleman, "Terahertz microfluidic sensor based on a parallel-plate waveguide resonant cavity," Appl. Phys. Lett. 95 (17), 171113 (2009).
[26] I. J. H. McCrindle, J. Grant, T. D. Drysdale, and D. R. S. Cumming, "Hybridization of optical plasmonics with terahertz metamaterials to create multi-spectral filters," Opt. Express 21(16), 19142-19152 (2013).
[27] R. Mendis, A. Nag, F. Chen, and D. M. Mittleman, "A tunable universal terahertz filter using artificial dielectrics based on parallel-plate waveguides," Appl. Phys. Lett. 97(13), 131106 (2010).
[28] B. S. Phillips, P. Measor, Y. Zhao, H. Schmidt, and A. R. Hawkins, "Optofluidic notch filter integration by lift-off of thin films," Opt. Express 18(5), 4790–4795 (2010).
[29] A. Yariv, Optical Electronics in Modern Communications (Oxford U. Press, Oxford, 2007).
[30] M. A. Ordal, R. J. Bell, R. W. Alexander, Jr, L. L. Long, and M. R. Querry, "Optical properties of fourteen metals in the infrared and far infrared: Al, Co, Cu, Au, Fe, Pb, Mo, Ni, Pd,Pt, Ag, Ti, V, and W," Appl. Opt. 24(24), 4493–4499 (1985).
[31] J. R. Birch, "The far-infrared optical constants of polypropylene, PTFE, and polystyrene," Infrared Phys. 33(1), 33–38, (1992).